agronomy

Article

CFD Simulation and Uniformity Optimization of the Airflow Field in Chinese Solar Greenhouses Using the Multifunctional Fan–Coil Unit System

Jiarui Lu, He Li, Xueying He, Chengji Zong, Weitang Song * and Shumei Zhao

College of Water Resources and Civil Engineering, China Agricultural University, Beijing 100083, China
* Correspondence: songchali@cau.edu.cn

Abstract: Supplying homogenous and suitable airflow schemes were explored in Chinese solar greenhouses, which had a positive impact on the crop yield and quality. This paper provided a multifunctional fan–coil unit system (FCU) to assist in circulating air. This system could collect the surplus heat of daytime air and release it to heat the greenhouse at nighttime. However, the main problem to be faced was the nonuniform airflow distributions. Thus, this paper aimed to optimize and analyze the placement strategy of the FCU system for a Chinese solar greenhouse using the numerical methodology. The computational fluid dynamics model was constructed to evaluate the effect of the FCU system on the airflow field and to uphold its validation. The complex structure of the FCU system was simplified to a fan model by fitting the pressure jump and the air velocity to enhance the practicality of the simulation model. Finally, the coefficient of variation was used to optimize four parameters: the tilt angle, swing angle, height above the ground, and shape of the outlet baffle. The effective disturbance velocity percentage was proposed as the evaluation index to improve the turbulence characteristics. The mean absolute error (MAE) between the measured and simulated values of the air velocity for the two planes was 0.06 m/s and 0.09 m/s, and the root mean square error (RMSE) was 0.08 m/s and 0.11 m/s. The simulated results showed that the coefficient of variation before optimization was 0.76, and the effective disturbance velocity percentages of the planes at 0.7 m and 1.0 m from the ground were 42.73% and 41.02%, respectively. After optimization, the coefficient of variation was reduced to 0.33, and the effective disturbance velocity percentages of the two planes increased to 58.68% and 43.73%, respectively. These results significantly improved the uniformity of the interior airflow field. This paper provides a reference for the design and installation of the FCU system.

Keywords: Chinese solar greenhouse; homogeneity; numerical simulation; airflow organization; installation parameters

Citation: Lu, J.; Li, H.; He, X.; Zong, C.; Song, W.; Zhao, S. CFD Simulation and Uniformity Optimization of the Airflow Field in Chinese Solar Greenhouses Using the Multifunctional Fan–Coil Unit System. *Agronomy* **2023**, *13*, 197. https://doi.org/10.3390/agronomy13010197

Academic Editor: Xiangjun Zou

Received: 13 December 2022
Revised: 3 January 2023
Accepted: 5 January 2023
Published: 8 January 2023

1. Introduction

A Chinese solar greenhouse (CSG) is a unique energy-saving and environment-friendly horticultural facility in Northern China which mainly relies on solar energy as the heat source [1,2]. This facility can achieve the overwintering production of vegetables without or with less heating in the winter. CSGs generally adopt the form of closed management during the winter to ensure a suitable interior temperature, which leads to airflow stagnation. The airflow organization can break the boundary layer of the leaves to promote photosynthesis and makes the temperature, humidity, and CO_2 concentration in the greenhouse uniformly distributed, which facilitates crop growth [3,4]. The suitable airflow range for crop growth is 0.2–1.0 m/s [4,5]. Therefore, the greenhouse air circulation is an important part of improving the growth environment and increasing the crop yield.

The circulation fan could enhance the convective airflow near the crop canopy during the operation condition, thus increasing the boundary layer conductance [6,7]. The application of circulation fans in greenhouses can be traced back to 1961 in order to regulate interior environmental uniformity. There are few specific studies on the effects of the different airflow distributions formed by the circulation fan on crops in the greenhouse industry. The first study on the different air supply methods of circulation fans was in 1974. Walker et al. [8] discussed the effects of a vertical air supply, horizontal air supply, and certain-angle air supply on the air velocity in a greenhouse. The results showed that the air distribution was optimal when the fan was deflected at 15° horizontally, which could meet the design requirements. In addition, the number, location, deflection angle, and operation combination form of circulating fans have a significant influence on the greenhouse microclimate [9,10]. Ishii et al. [11] found that 10 to 15 fans were required to generate an airflow above 0.3 m/s in a greenhouse of 1000 square meters. Tokairin et al. [12] suggested that arranging the additional fan when the air supply speed of the circulating fan dropped below 0.1 m/s could effectively improve the velocity attenuation problem. On this foundation, Tokairin et al. [13] concluded that the coupling effect of the height of the circulation fan from the ground and the air supply speed also affected the environmental conditions in the greenhouse. The experimental results showed that the disturbance effect was not obvious when the circulating fan system was installed at an excessive height, which was unfavorable to the regulation of the microclimate within the crop canopy. Previous studies have adopted a single circulating fan system to create a relatively appropriate growth environment for greenhouse crops. In recent years, more research has focused on the combined utilization of recirculating fans with other environmental control devices to achieve the improved regulation of the greenhouse environment. Air conditioning and circulation fans are the most widely employed environmental control devices, which are mainly used in plant factories. The combined application of circulation fans and air-conditioning equipment dramatically improves the airflow rates. There was one study that revealed that the combined usage of both devices increased the air flow rate by 24% compared to the separate usage of air conditioning, which contributed to the improvement of the temperature deviation between different culture beds. Furthermore, the lettuce indicators were determined through the experiment, and the fresh weight, leaf number, and leaf length increased by 40.6%, 41.1%, and 11.1%, respectively [14]. In the investigation of the combined use of internal and external circulation fans and air conditioning on the improvement of crop growth indicators, it was found that the effect of external circulation fans on the improvement of crop growth indicators was limited and that only the combined use of the three devices could optimally improve the effect [15]. For multispan glass and plastic greenhouses, there have been some studies on the combined use of circulating fan systems and evaporative cooling pad–fan systems [12,16,17]. These studies focused on the air supply direction of the two systems. When the circulating fan system and the evaporative cooling pad–fan system of the air supply direction were opposite, the air mixture on different planes was better, and the temperature distribution was more uniform. Additionally, the greenhouses with polycarbonate sheets as a covering material employed a combination of the circulating fan and the box evaporative cooler for heat removal [18]. In a nutshell, these studies have found that the air circulation from the circulating fans promoted the uniformity of the crop growth parameters in the whole greenhouse and effectively improved the relative humidity and temperature range of the crop-growing environment.

Most of the existing research on circulating fans has been conducted in glass and plastic greenhouses, and little research has been performed in CSGs. Duan et al. [19,20] arranged two internal circulation fans in a CSG and simulated the airflow and temperature fields formed by the fans at different locations using CFD techniques. It was found that the system could realize the air circulation and significantly improve the wind speed and temperature. In the follow-up research, Zhuang et al. and Zhang et al. [21,22] analyzed the installation height of a circulation fan in a CSG. The results showed that the application of circulating fans could improve the airflow velocity, and the installation height of the fans installed at 1 m to 2 m above the crop canopy produced the highest percentage of the airflow velocity in the effective disturbance range. However, the installation height was not determined through a detailed simulation analysis and was only selected due to the percentage of the effective disturbance velocity. Li et al. [23] proposed a fan–coil unit (FCU) active heat collection and release system that integrated a circulation fan with a water circulation heat storage and release module for their combined application. The FCU system was installed in a ridge inside a plastic greenhouse or CSG. The heat was collected and released through the coupling of the water-vapor heat exchange and forced convection. Therefore, the FCU system supported the effect of collecting and releasing heat while having a disturbing airflow to provide a certain amount of air speed for crop growth. After system optimization and upgrading, He et al. [24,25] concluded that the FCU system had a remarkable energy-saving effect and that the coefficient of performance was excellent. Different heat collection modes could be selected for different weather conditions. Zong et al. [26] also confirmed that the FCU system ensured the safe overwinter production of crops in cold weather after the experimental studies. However, the circulation fan inside the FCU system has the effect of a uniform airflow field during the process of air supply, but no attention has been attached to the homogeneity of the airflow field formed by this system.

The existing research on circulating fans has focused on its utilization to provide the appropriate air velocity to improve the greenhouse microclimate environment, but little research has been done on the uniformity of the airflow field. A uniform airflow field can provide a relatively consistent airflow for the crop canopy, which is conducive to stimulating the growth and development of the crops. Therefore, the main objective of this paper was to propose a novel predictive scenario-based installation parameter model using CFD techniques to aid in optimizing airflow uniformity. Solidworks software was used to construct the physical model, and the Fluent platform was applied to simulate the airflow fields. The numerical model was validated by the experimental measurements. By optimizing four factors, the tilt angle, swing angle, height above the ground, and shape of the outlet baffle, an installation scheme with an effective uniform airflow field was finally obtained. The aim of improving the airflow uniformity in the greenhouse could be achieved without any additional equipment or energy consumption simply by optimizing the installation parameters. This study could provide theoretical guidance for the installation and design of the system and could provide ideas for a uniform greenhouse environment.

2. Materials and Methods

2.1. Experimental Greenhouse

In order to demonstrate the model systematically, the experiment was conducted in Caoxian County of Heze City, Shandong Province, China (longitude 115.5° E and latitude 34.8° N). The experimental greenhouse span and ridge height were 10 m and 4.5 m, respectively. The east–west-oriented greenhouse was without a back wall of heat storage compared to traditional solar greenhouse. In the experiment, the crops grown in the greenhouse were low-growing leafy vegetables. The overall skeleton of the greenhouse consisted of an assembled structure of galvanized steel pipes. The north wall of the greenhouse was constructed of 130 mm thick polystyrene foam panels, while the east and west walls were composed of sintered bricks with a width of 370 mm. The south roof of the greenhouse was covered with 0.1 mm thick PO film. The outside of the film was covered with an insulating quilt at night in winter to reduce heat loss. As shown in Figure 1, a total of ten FCU systems were installed to regulate the thermal environment of the greenhouse in the absence of heat storage on the north wall. Based on earlier studies, each FCU system was separated evenly by 4 m and was empirically deployed under the ridge of the greenhouse.

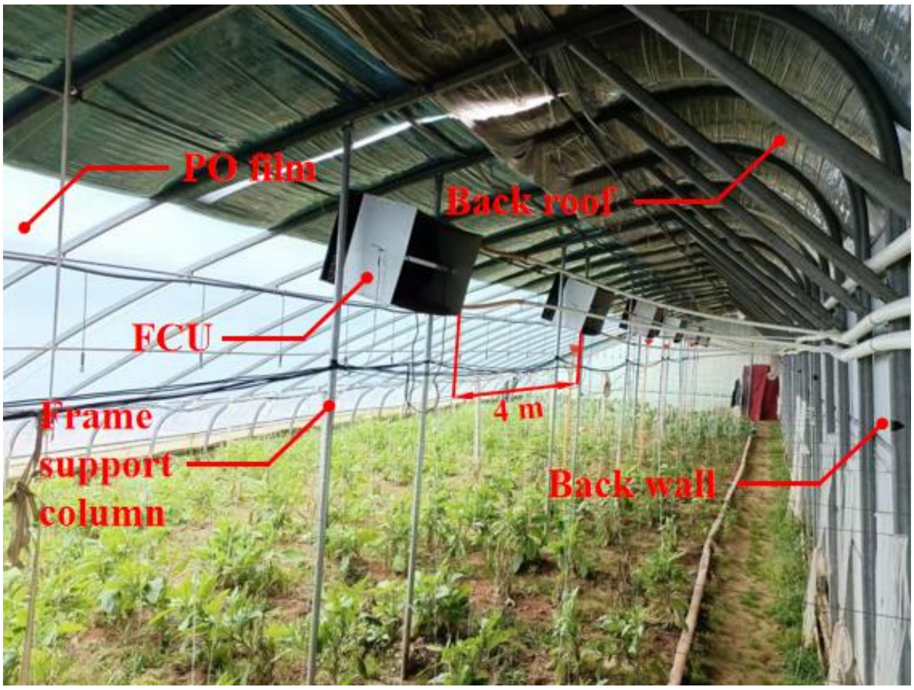

Figure 1. Layout diagram of FUC systems in experimental solar greenhouse.

2.2. Experimental Data Collection

In this experiment, two FCU systems with the same layout were selected randomly. The air velocity profiles at the outlet of the circulation fans were measured. The specific test method included dividing the air outlet into nine equal regions (Figure 2a). The air velocity of each measurement point was tested three times using a KANOMAX hot-wire anemometer (KA41, Kanomax, Japan), with a range of 0.10–30.0 m/s, a resolution of 0.01 m/s, and its accuracy ± 3%. The data were collected after sensor correction, and the average value was calculated. Finally, the outlet velocity of the circulation fan was obtained to provide the fitting variables for the simulated fan model. The velocity testing of individual circulation fan outlet assisted in reducing errors caused by fan-to-fan discrepancies.

To verify the accuracy of the model constructed in this paper, four vertical profiles (A, B, C, and D) were arranged equally between the FCU systems (Figure 2b). As depicted in Figure 2a, there were twenty measurement points for air velocity in each vertical profile. Moreover, the greenhouse was completely enclosed during the experiment, and the air flow was predominantly driven by the FCU systems. The field tests were conducted on a typical cloudy day in February 2022 to avoid the disturbing effect of thermal buoyancy on the greenhouse airflow. In addition, this paper also performed a preliminary analysis and found that the airflow distributions of the vertical section on different cloudy days were similar. Therefore, the arrangement of the FCU systems determined the flow pattern of the airstream organization.

2.3. CFD Numerical Simulation Method

2.3.1. Fundamental Control Equations

Computational fluid dynamics (CFD) is a common method to simulate the airflow pattern in horticultural facilities [27,28]. In this study, a steady-state numerical model was constructed to evaluate the effect of the FCU systems on the airflow field. CFD commercial software (Fluent 2020R1, ANSYS, New York, NY, USA) was applied for quantitative and qualitative analysis of air circulation characteristics. The 3D steady Reynolds-averaged Navier–Stokes (RANS) equations were performed in combination with the realizable k-ε turbulence model. The continuity and momentum conservation equations were described as Equations (1) and (2).

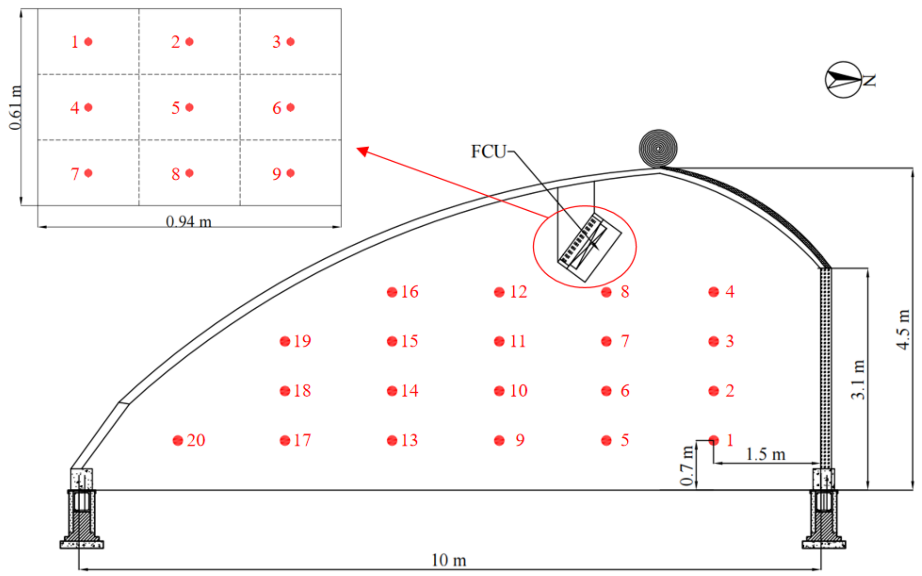

(**a**) Arrangement of fan outlets and vertical profile measurement points.

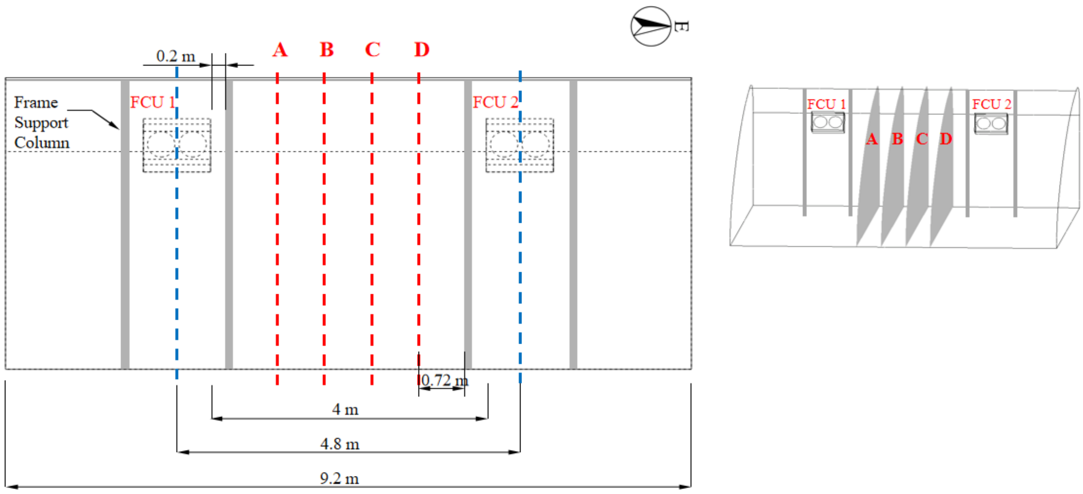

(**b**) Distribution of vertical profiles between the FCU systems.

Figure 2. Schematic diagrams of the two identical FCU systems and arrangement of the measuring points.

$$\nabla \cdot \vec{u} = S_{\mathrm{m}} \tag{1}$$

where $\vec{u}$ is the velocity vector of the computational domain (m s^{-1}) and where S_m is a user-defined source term.

$$\rho \vec{u} \cdot \nabla \vec{u} = -\nabla p + \left((\mu + \mu_T) \left(\nabla \vec{u} + (\nabla u)^{\mathrm{T}} \right) \right) + \rho \vec{g} \tag{2}$$

where ρ is the air density (kg/m^3), p is the pressure (Pa), μ is the dynamic viscosity (Pa s), μ_T is the turbulent viscosity, and $\vec{g}$ is the gravity acceleration vector (m/s^2).

Turbulence was modelled using the realizable k-ε turbulence model [29,30]. The incompressible gas law was employed as equation of state to link density. This realizable k-ε turbulence is a significant improvement over the standard k-ε model, allowing for more accurate predictions of flat, circular jets [31]. This is based on model transport equations for the turbulence kinetic energy (k) and the turbulence dissipation rate (ε) [5,32] as shown in Equations (3) and (4). Meanwhile, the standard wall function was also considered for the accuracy of near-wall airflow [33].

$$\rho \vec{u} \cdot \nabla k = \nabla \cdot \left(\left(\mu + \frac{\mu_T}{\sigma_k} \right) \nabla k \right) + G_k - \rho \varepsilon \quad (3)$$

$$\rho \vec{u} \cdot \nabla \varepsilon = \nabla \cdot \left(\left(\mu + \frac{\mu_T}{\sigma_\varepsilon} \right) \nabla \varepsilon \right) + G_{1\varepsilon} \frac{\varepsilon}{k} G_k - G_{2\varepsilon} \rho \frac{\varepsilon^2}{k} \quad (4)$$

where k is the turbulent kinetic energy (kg m^3); ε is the turbulent dissipation rate (kg m^2), G_k is the turbulent kinetic energy generated by the mean velocity gradient (N m), σ_k and σ_ε are the turbulent Prandtl numbers (σ_k = 1.0, σ_ε = 1.2), and $C_{1\varepsilon}$ and $C_{2\varepsilon}$ are the model constants.

2.3.2. Computing Domain and Mesh Dividing

In order to reduce the computational time of model convergence, the physical model was simplified as follows: (1) There were ten identical FCU systems uniformly installed throughout the greenhouse space, and two FCU systems were selected for geometric modeling to analyze the airflow distributions. This was beneficial for dramatically reducing the number of meshes and lowering the computational cost. (2) The structure of the coil heat exchanger in FCU systems was complex in order to serve the heat exchange. The aim of this paper was to analyze the airflow field in the greenhouse, so the coil heat exchanger was ignored. To reduce the calculation error, the fan model in Fluent was considered by fitting the pressure jump and the air velocity. Finally, the outlet air capacity of the circulating fans in the FCU systems was similar to that of the actual field test. (3) To enhance the practicality of the simulation model, the skeleton structure of the greenhouse was ignored, and the support columns beside the FCU systems were not regarded. (4) Since the greenhouse was cultivated with low-growing leafy vegetables during the experiment, the effect of crops on airflow was ignored.

According to the above simplification principles, the Solidworks software (Dassault systems, Velizy-Villacoublay, France) was used to create the geometric computational domain. The schematic diagram of the greenhouse incorporating two identical FCU systems is shown in Figure 3. The coordinate origin was defined as the center of the intersection between the back wall surface and the ground surface.

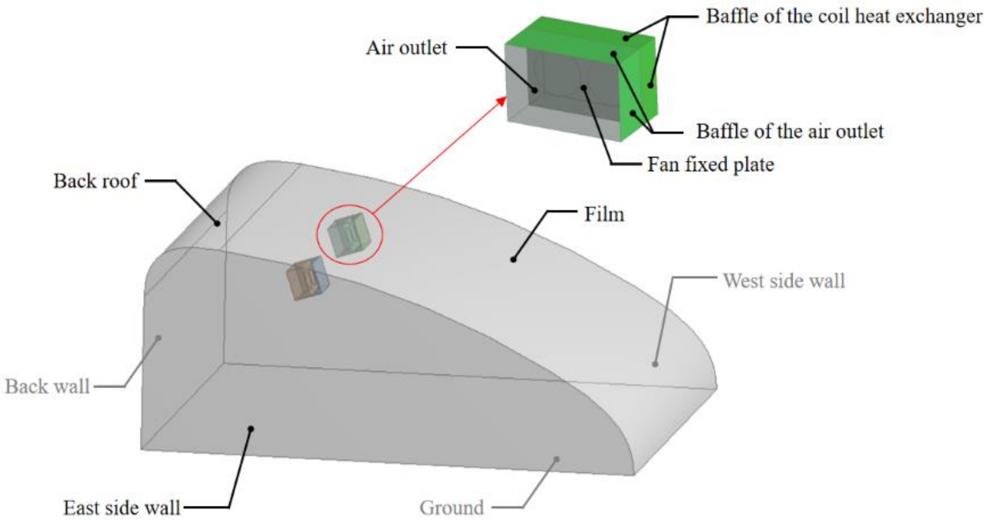

(**a**) Components of the computing domain.

Figure 3. *Cont.*

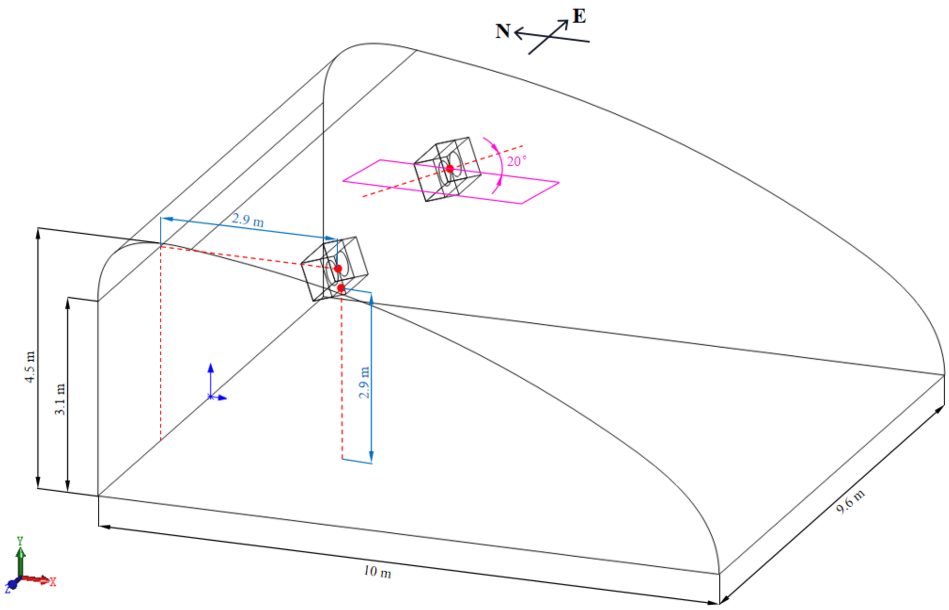

(**b**) Installation location of the FCU systems without optimized conditions.

Figure 3. Schematic diagrams of the greenhouse incorporating two identical FCU systems.

Based on the Fluent meshing module, the grid-dividing type of polyhexcore was chosen to analyze the greenhouse airflow field more accurately. The grid model with 696,883 cells is shown in Figure 4. The high-precision meshes were implemented on the fan baffle, the inlet, and the outlet of the fan model due to the large physical gradient near these locations. In this study, the average mesh skewness of the CFD model was less than 0.35, and the orthogonal quality was greater than 0.60, which was satisfactory.

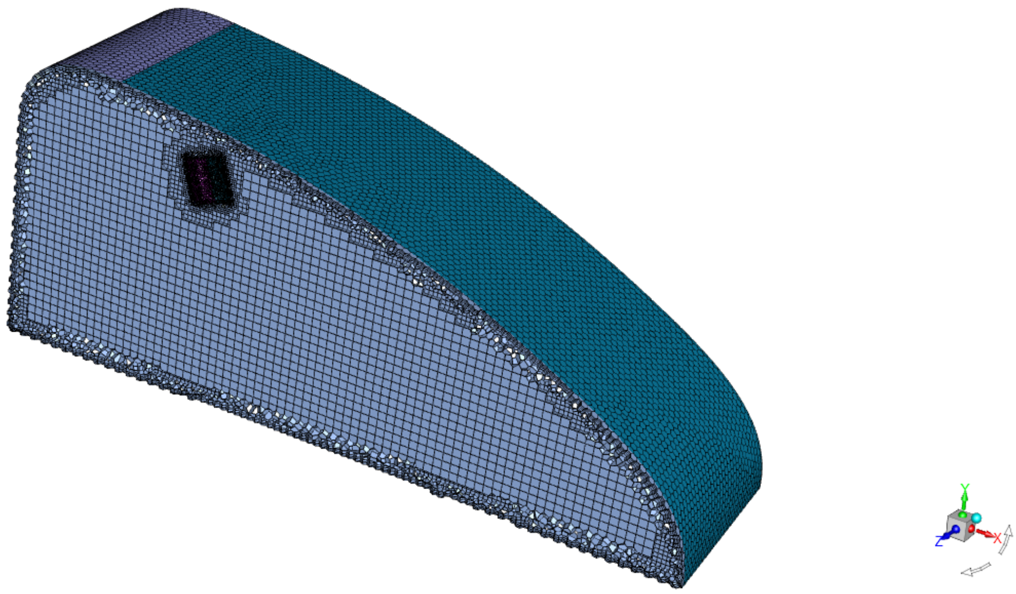

Figure 4. Computational grids used for the CFD simulation.

2.3.3. Boundary Conditions and Numerical Solution Process

In this study, the numerical calculation of the airflow fields was performed using a realizable k-ε turbulence model with an air density of 1.225 kg/m^3 and a gravitational acceleration of 9.81 m/s^2. There were ten FCU systems in the experimental greenhouse, where any adjacent systems interacted to form airflow fields that were identical. Therefore, the purpose of setting the east and west side walls of the calculation domain as symmetrical boundary conditions was to reduce the large space to a limited space, thereby improving the computational efficiency [34]. The boundary condition settings for the simulation model are shown in Table 1. The pressure-jump range in the fan model was set from 1 to 10 Pa, and the simulated fan outlet velocity values were fitted. The relationship between pressure jump and fan outlet velocity was described as Equation 5, and the nonlinear fitting results are shown in Figure 5. The experimentally measured fan outlet velocity was 1.53 m/s, and the pressure jump of the fan model was derived to be 3.2 Pa. In the Fluent fan model, the pressure jump of two identical fans in the computational domain was adjusted to 3.2 Pa, and the calculation was performed again. The calculated outlet velocity obtained from the simulation was 1.54 m/s with a relative error of 0.65% from the experimental average value of 1.53 m/s. It can be seen that the boundary conditions of the fan model were set up reliably.

$$\Delta P_{fan} = 1.12{u_{outlet}}^{0.27} \tag{5}$$

where ΔP_{fan} is pressure jump (Pa) and where u_{outlet} is the fan outlet velocity (m/s).

Table 1. Boundary conditions for the simulation model.

Parameter	Boundary Conditions
Fan–coil units	The fan model
Back wall	Nonslip wall
Back roof	Nonslip wall
Film	Nonslip wall
Ground	Nonslip wall
East and west walls	Symmetry
Baffle	Nonslip wall
Fixed plate	Nonslip wall
Inlet and outlet of the fan–coil units	Interior

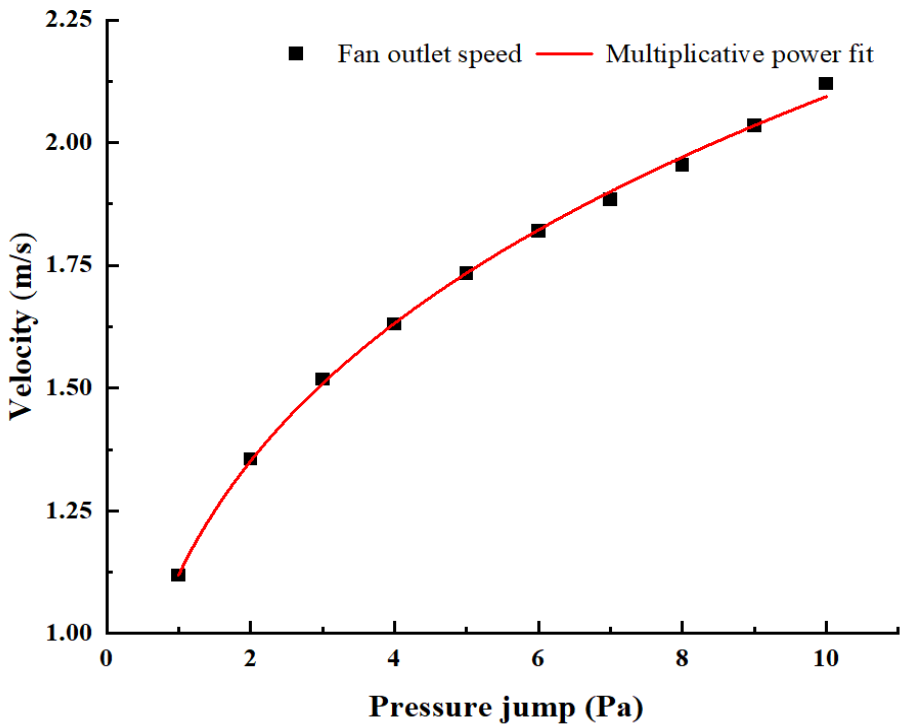

Figure 5. Diagram of pressure jump versus fan outlet velocity.

This paper conducted simulation using ASUS laptop with 8-core 3.2 GHz AMD processor, 16G RAM, and Windows 10 64-bit operating system. The steady-state method was employed for the calculations, and the coupled algorithm was adopted for the pressure–velocity solver. The second-order upwind format was used to discretize the momentum equation, and the turbulent kinetic energy (k) and turbulent dissipation rate (ε) equations were calculated using a first-order upwind format. The pseudotransient calculation was turned on in the calculation to facilitate convergence. The residual settings for the continuity, momentum and turbulence equations were all set to the default value of 10^{-3}. The number of simulation calculation steps was set to 1000 steps. Additionally, the average body velocity of the computing domain was monitored during the simulation, and it tended to be stable and constant within 1000 steps; this implies that the calculation could be judged to have reached a convergence state.

2.4. Evaluation Indexes for CFD Model Validation

The measured and simulated values of a total of forty monitoring points in vertical profiles were compared using two evaluation indexes, including root mean square error (RMSE) and mean absolute error (MAE). The RMSE can visually evaluate the data discreteness, and smaller values indicate that the prediction model describes the experimental data with higher accuracy. The MAE can better reflect the actual situation of the prediction value error. The RMSE and the MAE equations are shown below:

$$RMSE = \sqrt{\frac{\sum_{i=1}^{N}(D_m - D_s)}{N}} \tag{6}$$

$$MAE = \frac{\sum_{i=1}^{N}|D_m - D_s|}{N} \tag{7}$$

where D_m and D_s are the measured and simulated values of each monitoring point and where N is the number of monitoring points.

2.5. Optimization Program for Simulation Models

2.5.1. Optimization Factors and Methodologies

The installation parameters of the FCU systems included five components, including the fan upper and lower tilt angle (i.e., the angle between fan axial and greenhouse horizontal surface), the fan left and right swing angle (i.e., the angle between fan axial and greenhouse vertical surface), the fan height from the ground, the fan distance from the back wall, and the baffle shape of the outlet of FCU systems. In the experimental greenhouse without optimized FCU systems, the distance of this system to the back wall was specified to be the equivalent of the distance from the top vent to the back wall. The reason for this was to ensure that the circulation fan in the system had a favorable air intake when the greenhouse was not completely closed. In addition, this also guaranteed sufficient heat collection in the daytime. Therefore, this paper mainly extracted four factors to optimize the fan installation parameters, including the fan tilt angle, swing angle, height from the ground, and baffle shape. A single factor analysis was performed to elaborate the impact of the four factors. The geometric models for different optimization scenarios were constructed using Solidworks, and the procedures for geometry naming, mesh dividing, and simulation calculations were identical.

2.5.2. Optimization Monitoring Point Arrangement

Based on the study of velocity distributions in the vertical plane (plane A and plane C), in the optimization part of the airflow field, another four horizontal planes of different heights from the ground (0.7 m, 1.0 m, 1.3 m, and 1.6 m) were selected for optimization analysis, which is shown in Figure 6.

The ANSYS CFD-Post module was used to postprocess the results of the CFD simulation. The collection of velocity data was concentrated on four horizontal planes within the crop growth height. Each target horizontal plane was assigned 18 data points, and the four horizontal planes were separated with equal spacing of 0.3 m. As shown in Figure 7, the velocity data collection in four optimization target planes focused on the values of the velocity below the FCU central axis (a, f) and on the four lines (b, c, d, e) that were equally spaced between the FCU systems.

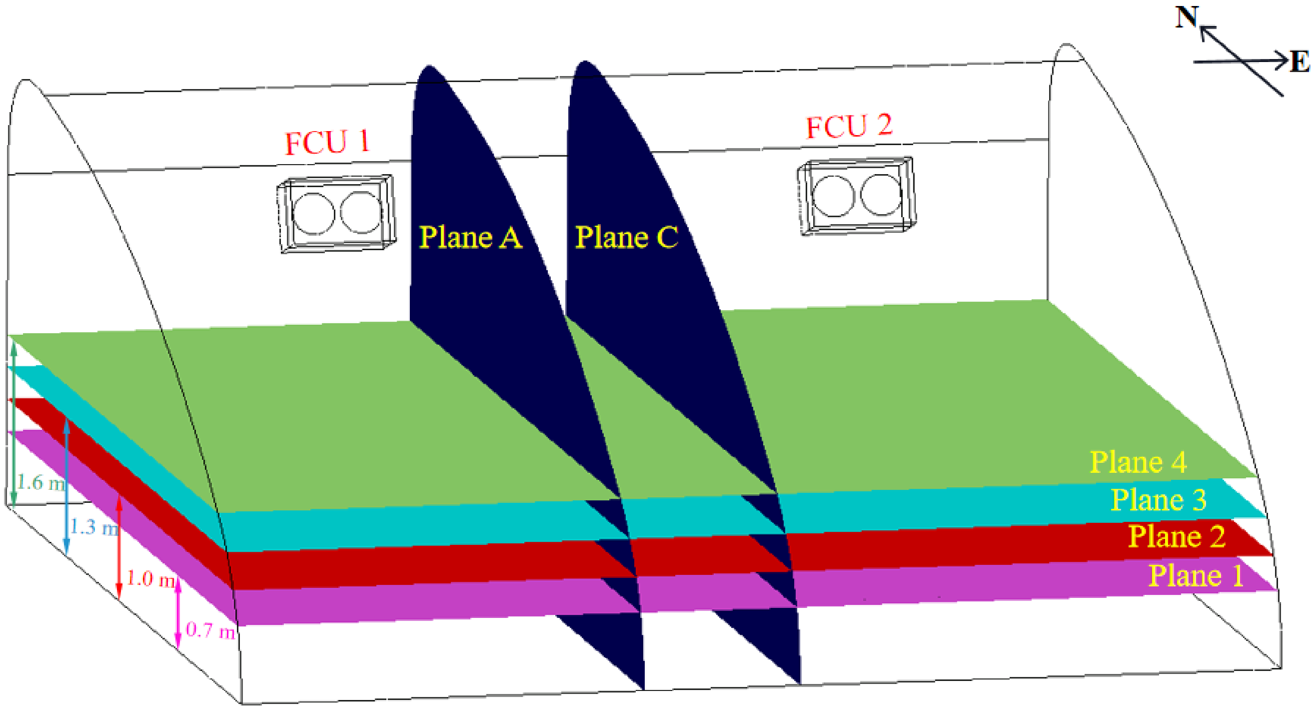

Figure 6. Layout of optimization target plane.

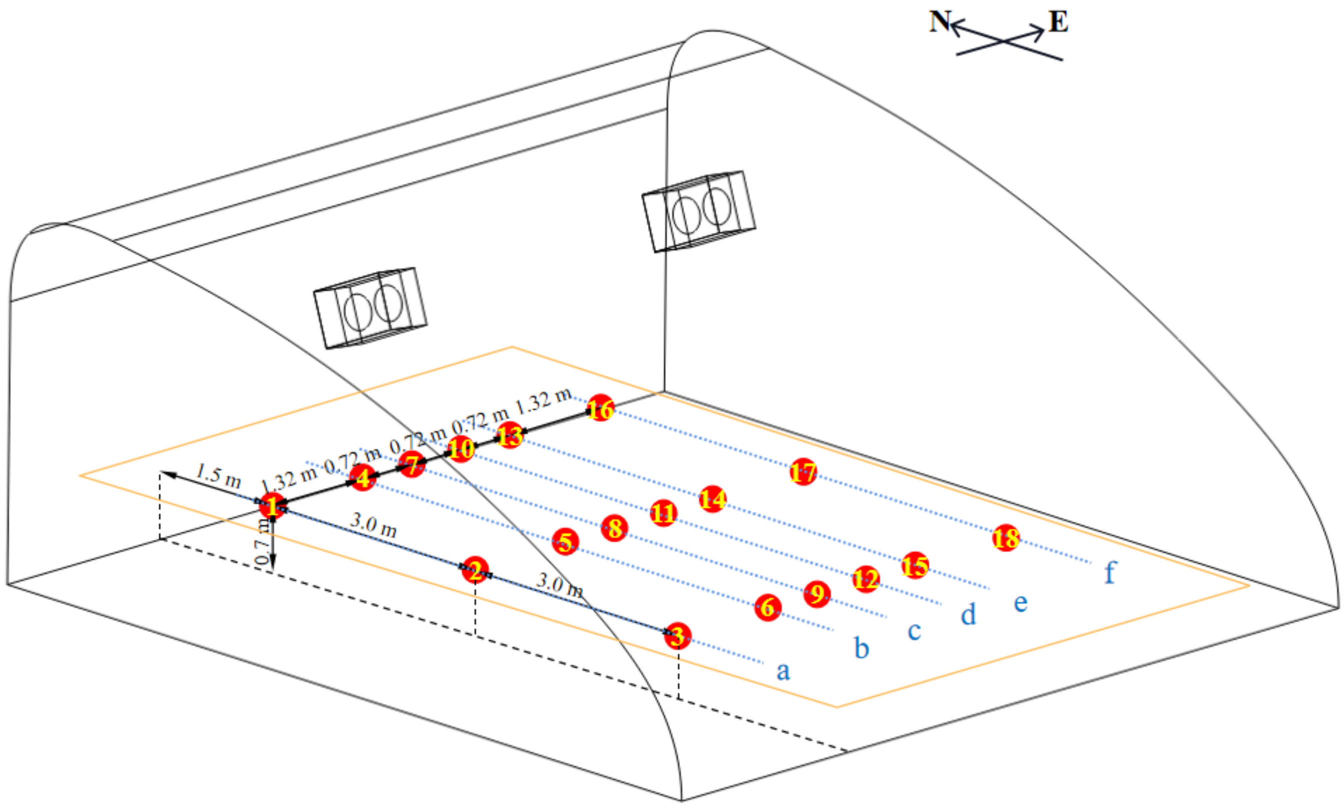

Figure 7. Layout of data collection points in the optimization target plane.

2.5.3. Evaluation Criteria for Optimized Schemes

The evaluation criteria for optimized schemes was the coefficient of variation (C_v) as shown in Equation (8). The coefficient of variation takes values from 0 to 1. Smaller values signify a better uniformity of the airflow distribution. In actual productions, microclimate homogeneity in crop areas tends to receive more attention [35,36]. Therefore, the coefficients of variation of planes 1 to 4 were derived sequentially after obtaining the simulation data. The average value of four optimization target planes was employed to represent the overall homogeneity of the velocity distribution within the crop area in the greenhouse space.

$$C_v = \frac{1}{\overline{u}}\sqrt{\frac{\sum_{i=1}^{N}(u_i - \overline{u})^2}{N}} \tag{8}$$

where $\overline{u}$ is the average of airflow velocities of N collection points (m/s) and where u_i is the airflow velocity of a collection point (m/s).

3. Model Validation and Optimization Scheme Analysis

3.1. Model Validation

As shown in Figure 2, the airflow simulation values of the measurement points in planes A, B, C, and D were compared with the experimental values for verification. When the swing angle of the FCU systems was 0°, planes A and D and planes B and C were two sets of symmetry planes, and the trials found that the air velocity at the measurement points in the symmetry planes had the same regularity. Therefore, planes A and C were selected for the model validation and optimization scheme analysis.

The comparison of the measured and simulated results for the measurement points in planes A and C is shown in Figure 8, and it can be seen that the overall tendency of the measured and simulated results in both the planes was the consistent. A few measurement points close to the film had an error close to 50%. This was due to the presence of the skeleton structures and horizontal columns. The length of the skeleton cross-section was 7 cm, and the width was 5 cm. The column was 10 cm from the film, and the diameter was 2.5 cm. The complex structures had an impact on the flow direction of the prevailing airflow. Since the model was simplified, the simulated velocity values showed a certain deviation from the measured values. The simulated value was higher than the measured value in a large number of cases. The main reason for this was that the air velocity in the whole greenhouse was quite small throughout the experiment period. There were deviations in the hot-wire anemometer for measuring the air velocity, and the recorded velocity was directional. Meanwhile, there were also partial measurement points in planes A and C where the simulated values were smaller than the measured values. The main reason for this was that small disturbances caused a fluctuation in the measured velocity. Furthermore, the heat exchanger coil of the FCU systems had a certain obstructive effect on the fan outlet airflow in the actual experiment. Thus, these unavailable errors caused a slightly offset airflow generation, with the airflow not blowing directly towards the front film but diffusing directly downwards. The RMSE between the simulated and measured airflow velocities in plane A and plane C was 0.08 m/s and 0.11 m/s, and the MAE was 0.06 m/s and 0.09 m/s. In general, the CFD simulated model had a strong correlation. In previous studies on simulating greenhouse airflow fields, RMSE and MAE values of measured and simulated airflow velocities that were below 0.128 m/s and 0.107 m/s were considered highly acceptable values [37,38]. Therefore, the numerical simulation based on the CFD method was suitable for analyzing the airflow field formed by the FCU systems in the solar greenhouse due to its strong correlation and practicability.

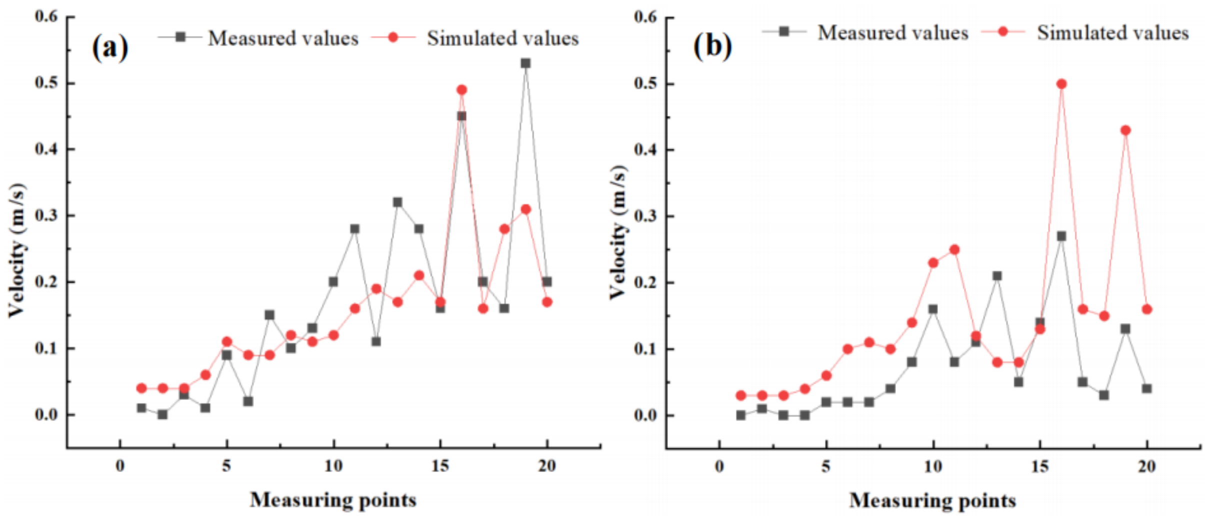

Figure 8. Comparison of measured and simulated velocity values of plane A (**a**) and plane C (**b**).

3.2. Analysis of Velocity Distributions before Optimization

The velocity distributions of the vertical profile of the solar greenhouse equipped with the FCU systems is shown in Figure 9. Plane A was close to the FCU system, and the maximum velocity of the profile was 1.04 m/s. It can be seen from Figure 9a that the airflow from the exhaust fan to the film surface could not be moved slowly along the film to the south edge. Instead, it blew down to the ground at 1.5 m away from the front bottom corner and then streamed along the ground towards the back wall, resulting in a back flow. There was a pronounced velocity gradient in the northern reflux region due to the more prevalent streamflow in plane A; plane C was far from the FCU system, and the maximum velocity of the profile was 0.75 m/s. Plane C had a smaller prevailing airflow than plane A. The airflow adjacent to the film flowed along the film surface to the bottom corner of the south side of the greenhouse. The prevailing airflow was mainly concentrated in the front foot of the greenhouse in the form of vortices (Figure 9b). In addition, the circulating airflow in the region of the south side of the two planes was generated by the superposition of the flow fields of the two identical fan models. It also can be seen from Figure 9 that the velocity distributions in both planes were extremely nonuniform. The airflow stratification in the horizontal height was not obvious for planes A and C, while the north–south direction was clear. Therefore, the empirical layout of the FCU system rendered it unfavorable for vegetables to grow evenly.

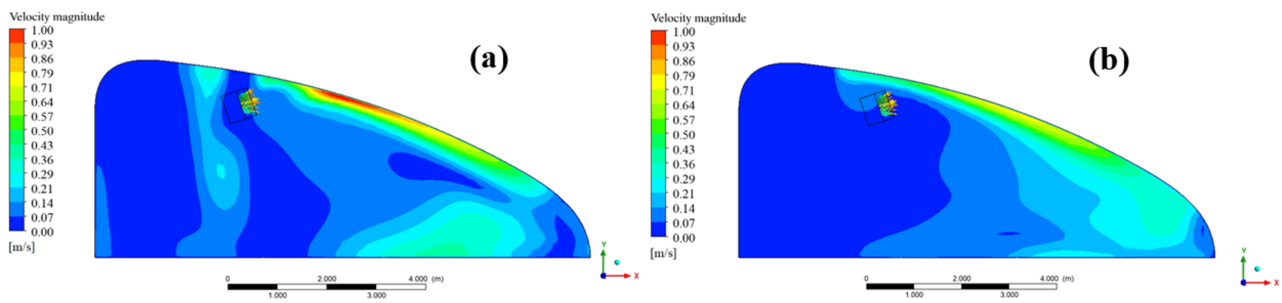

Figure 9. Velocity distribution contours for vertical profiles: plane A (**a**) and plane C (**b**).

Figure 10 shows the airflow velocity distribution contours for the four horizontal profiles (plane 1 to plane 4). Since the FCU systems were arranged at a fan tilt angle of 20°, the prevailing airflow from the air outlet immediately reached the front film and spread around the film as it migrated downwards. Therefore, the flow velocities ranged from 0.07 m/s to 0.49 m/s for the horizontal profiles adjacent to the greenhouse south side, where the values were higher. However, the airflow diffusion disturbance in the regions between the individual fans that were close to the back wall was weak owing to the approximate airflow velocity of zero. When the airflow moved down along the film, a minor portion of the airstream blew downwards from the south side of the 1.5 m position to the ground and moved northwards (similar to Figure 9a). Meanwhile, most of the remaining airflow moved northwards until it reached the south front bottom corner. The airflow velocity reaching the north side was largely reduced due to the distance constraint and the viscous force of the air surrounding the film. This led to a reduction in the airflow velocity range of up to 0.02–0.13 m/s when approaching the north wall. In addition, the prevailing airflow in the greenhouse's south area increased with a height above the ground based on the velocity distribution contours. The reason for this was attributed to the gradual decline in the velocity during the downward spread of the high-speed airflow. In a nutshell, the simulation results of the unoptimized system showed that the average airflow velocity of the four horizontal profiles was estimated to be 0.14 m/s, with velocity fluctuations in the range of 0.07–0.26 m/s, which suggested that the arrangement of the system required improvement.

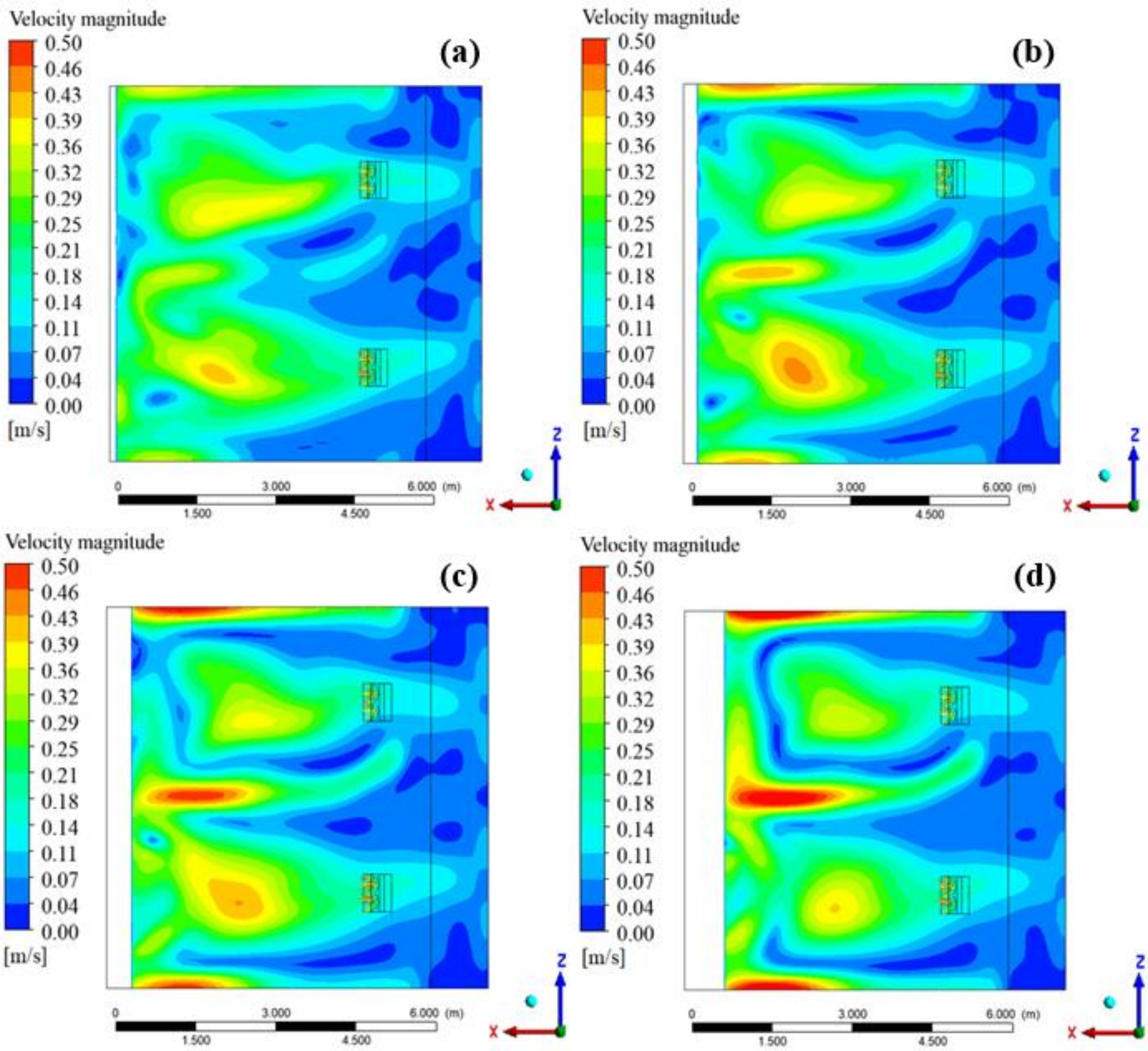

Figure 10. Velocity distribution contours for four horizontal profiles: plane 1—0.7 m (**a**), plane 2—1.0 m (**b**), plane 3—1.3 m (**c**), and plane 4—1.6 m (**d**).

3.3. Analysis of the Optimized Velocity Distribution

3.3.1. Fan Tilt Angle Optimization

When optimizing the fan tilt angle, the fan swing angle was 0°, the fan height from the ground was 2.9 m, and the baffle shape was set up as the rectangular frame structure.

In this paper, the fan tilt angle was specified to be a positive value for an upward tilt and a negative value for a downward tilt. After the simulation results of the airflow fields of the five cases were obtained, the postprocessing software was used to extract the velocity values of the 18 collection points in each horizontal profile. The coefficients of variation of the four horizontal profiles were calculated, and the average value of the four profiles is shown in Table 2. It can be seen that the coefficient of variation of the unoptimized model was 0.76. When the fan tilt angle was −70°, the coefficient of variation was 0.52.

Table 2. Summary of the coefficients of variation of horizontal velocity profiles for different fan tilt angles.

Emulated Scenarios	Fan Tilt Angle (°)	Coefficient of Variation
Case 1	+20	0.76
Case 2	−2.5	0.56
Case 3	−25	0.93
Case 4	−47.5	0.64
Case 5	−70	0.52

Figures 11 and 12 display the velocity clouds for the vertical and horizontal profiles when the fan tilt angle was −70°, respectively. The fan outlet in this case was arranged facing downwards, and the outlet airflow blew directly to the fan bottom areas. The disturbance flow velocity in this region ranged from 0.19 m/s to 0.56 m/s, and almost the majority of the prevailing airflow was concentrated. When the high-speed airflow impacted the ground, it contributed to the diffusion directly in the surrounding directions. Therefore, it can be seen that the velocities were higher near the east–west sides and north wall (0.13–0.26 m/s). Meanwhile, the fluctuating airflow between two individual fans (0.17–0.29 m/s) was created due to the mutual interference and overlap of the airflow fields. Figure 12 also reveals that the airflow diffusion range was wider near the ground and that the airflow superposition was more noticeable due to the impulse of the prevailing airflow. On the other hand, it is clear from Figure 11 that there was a large disparity in the velocity distributions between the two vertical profiles. The reason for this discrepancy was that plane A was 0.72 m closer to the FCU system than plane C, resulting in the velocity magnitude and airflow distribution zones being superior. Based on the simulation results, the average airflow velocity values of the four horizontal profiles were 0.14 m/s, 0.15 m/s, 0.15 m/s, and 0.14 m/s, respectively, with velocity fluctuations in the range of 0.04–0.14 m/s (Figure 12). Therefore, the adjustment of the fan tilt angle to −70° only favored improved uniformity, while the overall airflow velocity inside the greenhouse remained low.

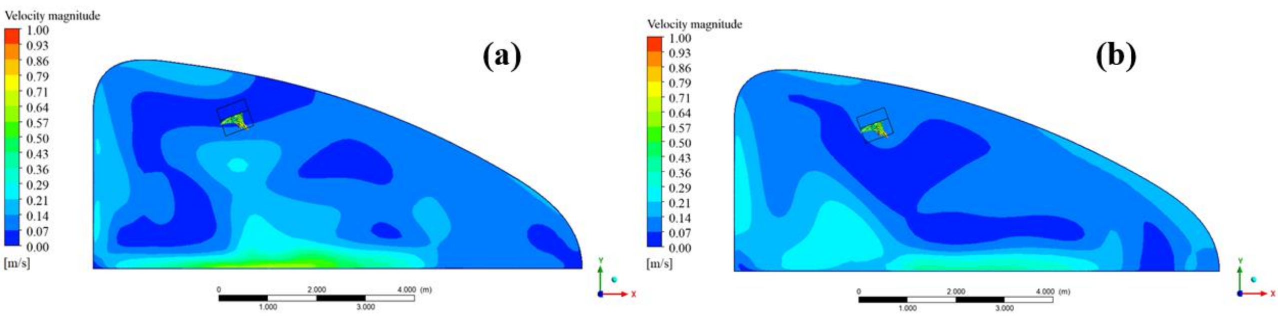

Figure 11. Velocity distribution contours for vertical profiles when the fan tilt angle was −70°: plane A (**a**) and plane C (**b**).

When the fan tilt angle was −2.5°, the coefficient of variation was 0.56. Figures 13 and 14 display the velocity clouds for the vertical and horizontal profiles, respectively. As observed previously in Figures 9 and 10, the airflow patterns under this case were similar to those without the optimization of the system layout parameters. The comparison showed that the main difference was that the tilt angle of the fan arrangement was downward. The airflow blew out from the fan outlet at an acceptable velocity and spread forward into the jet regime. After spreading forward for a certain distance, the airflow moved down along the film until it reached the greenhouse's south side and then switched directions to proceed along the ground to the north side. The airflow velocity gradually slowed down in the backflow process, making the obvious velocity stratification in the horizontal height. However, by comparing the velocity contours in Figures 9, 10 and 13, Figure 14, it can be seen that the north-side airflow velocity (0.02–0.22 m/s) was larger than that without optimization (0.02–0.13 m/s), and the airflow disturbance range was broader. This was attributed to the fact that the fan tilt angle was negative. Due to this, the airflow blew out and moved for a period of time before impacting the film, and the momentum consumption of the airflow was less than when it was not optimized. Eventually, when the fan tilt angle was −2.5°, the air velocity range between the two regulated fans was 0.03–0.17 m/s, which had a magnitude similar to that of the unoptimized condition. The average airflow velocity values of the four horizontal profiles were 0.19 m/s, 0.17 m/s, 0.16 m/s, and 0.16 m/s, respectively, with velocity fluctuations in the range of 0.09–0.34 m/s. Therefore, a fan tilt angle of −2.5° was better than that of −70° in terms of the canopy airflow magnitude for a similar uniformity.

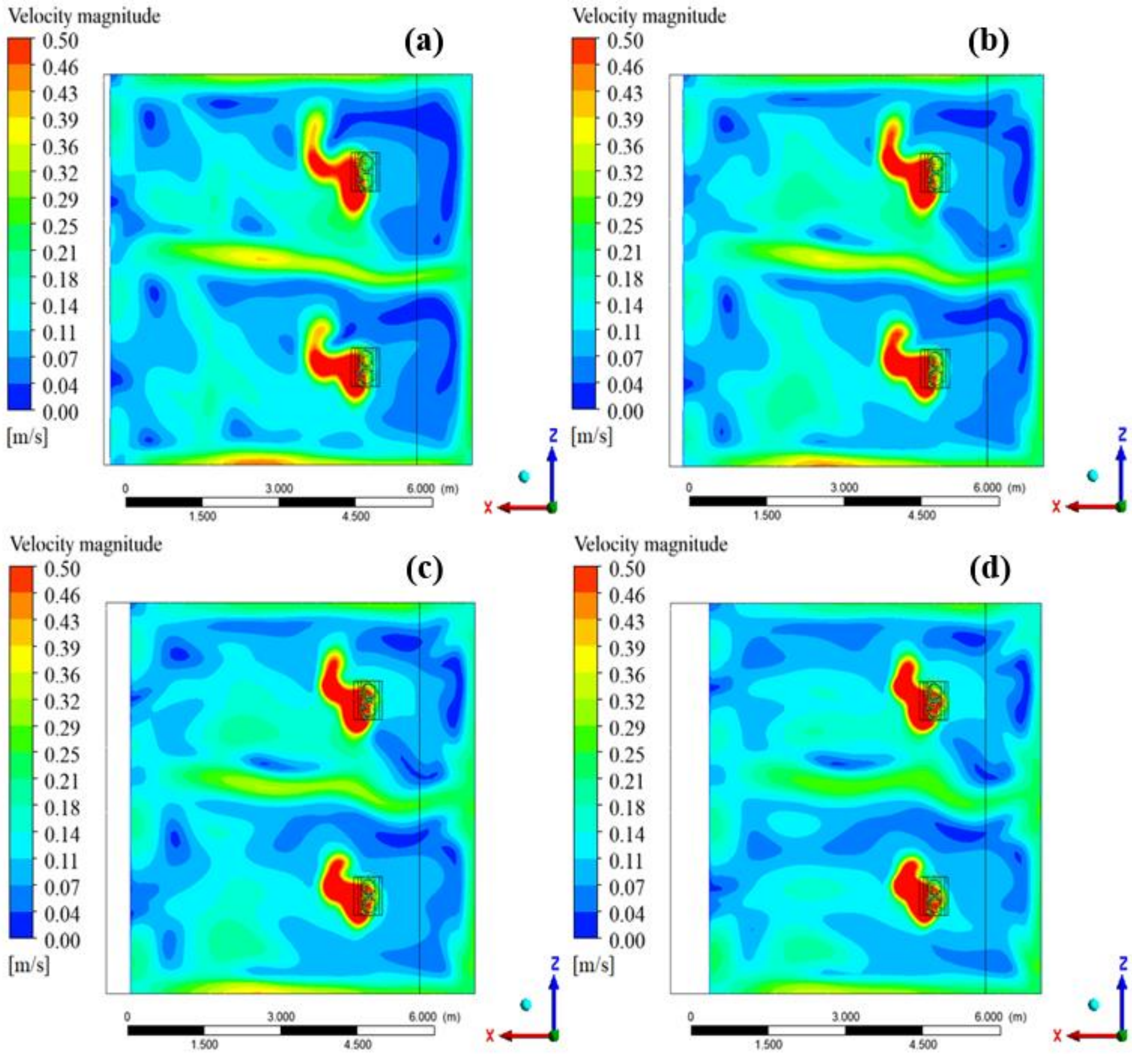

Figure 12. Velocity distribution contours for four horizontal profiles when the fan tilt angle was −70°: plane 1—0.7 m (**a**), plane 2—1.0 m (**b**), plane 3—1.3 m (**c**), and plane 4—1.6 m (**d**).

3.3.2. Fan Swing Angle Optimization

When optimizing the fan swing angle, the fan tilt angle was −2.5°, the fan height from the ground was 2.9 m, and the baffle shape was the rectangular frame structure. In consideration of the uniformity of the airflow fields formed by the identical fans, the swing angle of the individual fans was deviated by the equal angle to the same direction. Moreover, the airflow distribution patterns were similar for both of the FCU systems at equal swing angles offset to the west or east due to the greenhouse length being considerably longer than greenhouse span. Therefore, the fan swing angle was designed to take the eastward side into account only in the optimization process of this paper. The coefficients of variation of the airflow field for the five cases were calculated as shown in Table 3.

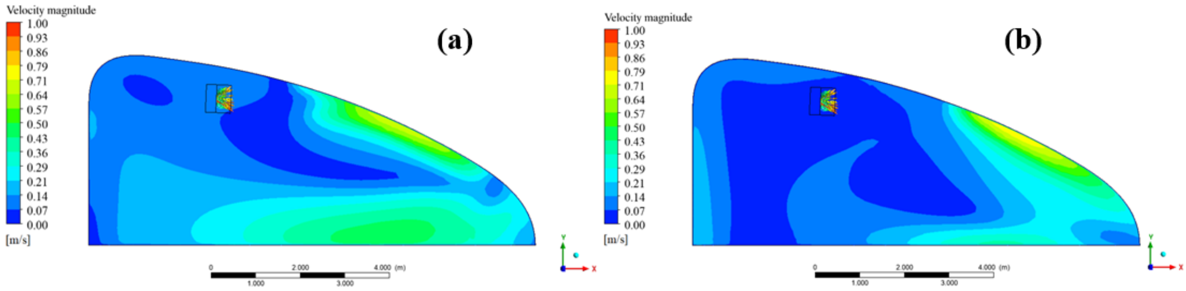

Figure 13. Velocity distribution contours for vertical profiles when the fan tilt angle was −2.5°: plane A (**a**) and plane C (**b**).

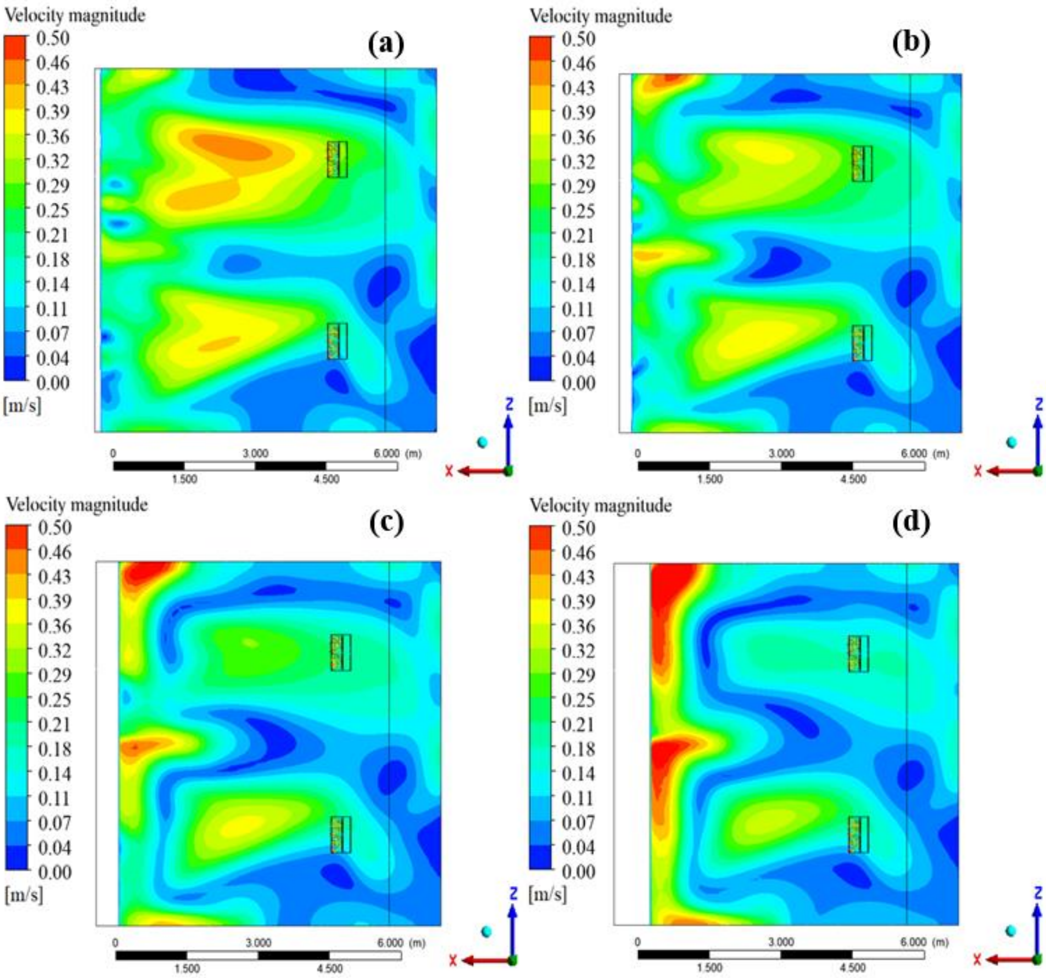

Figure 14. Velocity distribution contours for four horizontal profiles when the fan tilt angle was −2.5°: plane 1—0.7 m (**a**), plane 2—1.0 m (**b**), plane 3—1.3 m (**c**), and plane 4—1.6 m (**d**).

Table 3. Summary of the coefficients of variation of horizontal velocity profiles for different fan swing angles.

Emulated Scenarios	Fan Swing Angle (°)	Coefficient of Variation
Case 1	0	0.56
Case 2	15	0.72
Case 3	30	0.42
Case 4	45	0.58
Case 5	60	0.34

As can be seen from Table 3, the coefficient of variation for a fan swing angle of 60° was 0.34, which was the optimal scheme among the five cases. By comparing Figures 13 and 15, it was observed that both vertical planes had a noticeable velocity stratification at the horizontal height (Figure 15), whereas only plane A had a clear velocity gradient in Figure 13. In addition, the coefficient of variation decreased from 0.56 to 0.34, indicating that the airflow disturbance was more uniform throughout the space when the fan swing angle was adjusted to 60° as revealed in Figures 14 and 16. The uniformity of the area between the two fans was also visibly improved, and the optimized velocity range in this area increased from 0.03–0.17 m/s to 0.09–0.26 m/s. This occurred because the entire area scanned by the jet stream blowing out of the outlet was markedly expanded. Moreover, the uniformity of the airflow organization near the north wall of the greenhouse was somewhat improved. The average airflow velocity in the northeast corner region (0.09–0.16 m/s) was greater than the previous solutions (0.04–0.10 m/s). Ultimately, the average airflow velocity values of the four horizontal profiles were 0.18 m/s, 0.15 m/s, 0.13 m/s, and 0.13 m/s, respectively, with velocity fluctuations in the range of 0.10–0.33 m/s. From the average velocity in the four horizontal profiles, it was clear that the profile further from the ground had a smaller velocity, which was expected due to the production practice. In conclusion, a fan swing angle of 60° was further selected for subsequent optimization due to its acceptable airflow organization and uniform distribution characteristics.

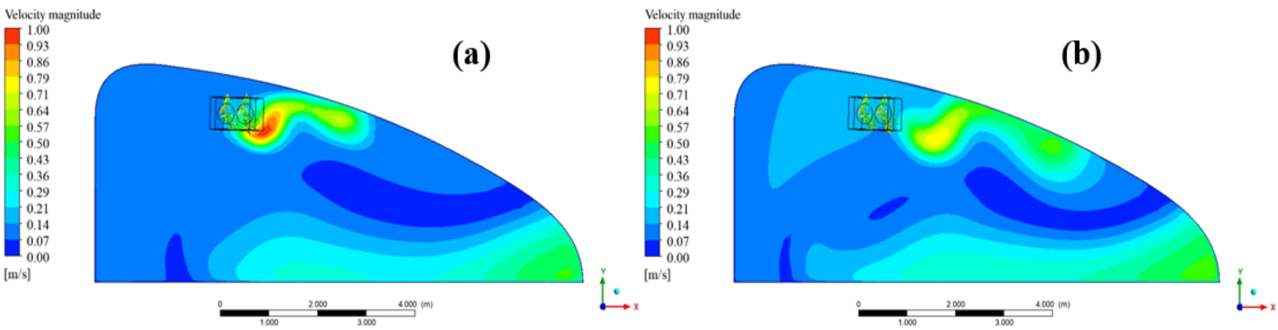

Figure 15. Velocity distribution contours for vertical profiles when the fan swing angle was 60°: plane A (**a**) and plane C (**b**).

3.3.3. Fan Height Optimization from the Ground

When optimizing the fan height from the ground, the fan tilt angle was −2.5°, the fan swing angle was 60°, and the baffle shape was the rectangular frame structure. In this paper, the optimized range of the height above the ground was 2.5–2.9 m after the comprehensive consideration of the crop canopy height. Furthermore, it was detected that the coefficient of variation was larger the closer to the ground it was and smaller the farther away from the ground it was based on the simulation analysis, and this trend is described in Table 4. The emergence of this phenomenon was due to the airflow's downward diffusion being more adequate when the fan was installed in a higher position, facilitating the retention of the stable airflow field. When the fan height above the ground was 2.9 m, the minimum coefficient of variation was 0.34. The airflow field distributions under this condition are shown in Figures 15 and 16. Therefore, the installation position of the fan at 2.9 m above the ground was confirmed and served for the subsequent optimization.

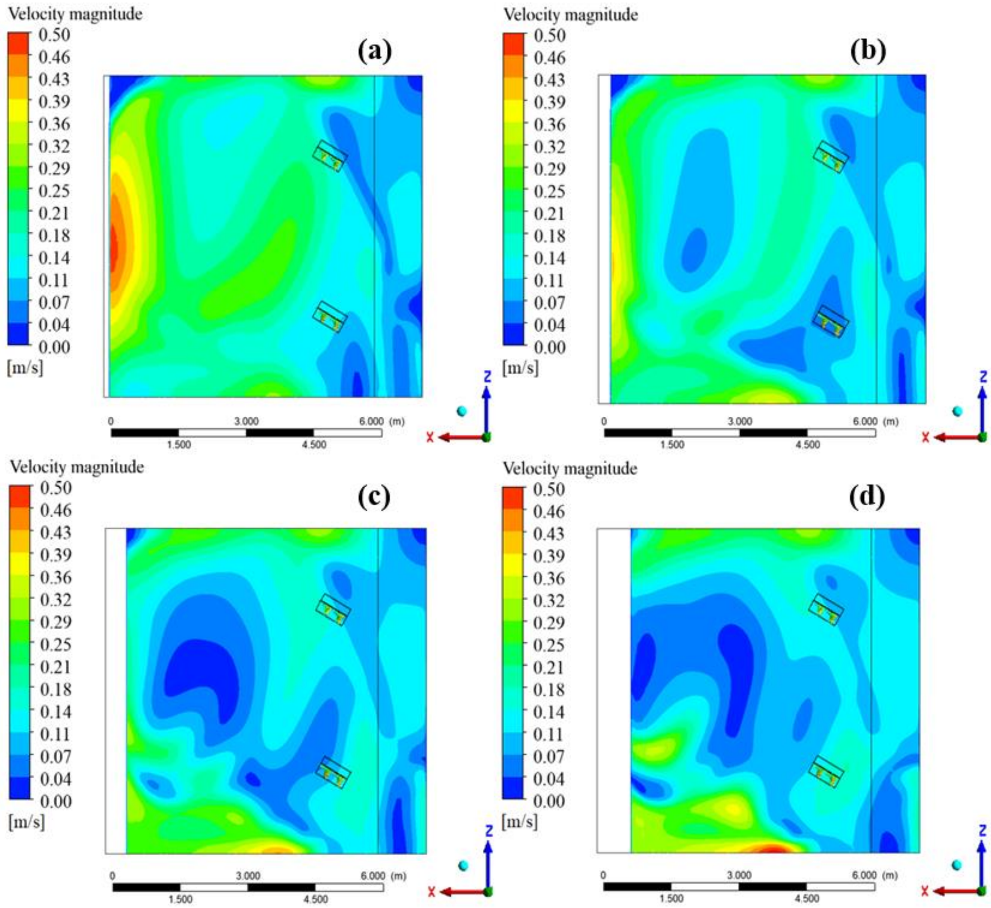

Figure 16. Velocity distribution contours for four horizontal profiles when the fan swing angle was 60°: plane 1—0.7 m (**a**), plane 2—1.0 m (**b**), plane 3—1.3 m (**c**), and plane 4—1.6 m (**d**).

Table 4. Summary of the coefficients of variation of horizontal velocity profile for different fan heights.

Emulated Scenarios	Fan Heights (m)	Coefficient of Variation
Case 1	2.5	0.38
Case 2	2.6	0.38
Case 3	2.7	0.37
Case 4	2.8	0.35
Case 5	2.9	0.34

3.3.4. Baffle Shape Optimization of the Fan Outlet

Figure 17 displays the rectangular frame structure for the fan outlet baffle in the experimental greenhouse. In this paper, we considered the influences of the baffle shape on the airflow diffusion and designed the flared fan baffle structure to assist the airflow diffusion. The opening angle of the upper baffle was restricted since the fan was close to the greenhouse roof. Therefore, the upper and lower opening angles of the outlet baffles were designated as 0°, 15°, and 30°, respectively. The left and right opening angles of the outlet baffles were designed as 0°, 15°, 30°, 45°, and 60°, respectively. Finally, the fourteen baffle optimization schemes were proposed as shown in Table 5. It can be observed that case 4 had the smallest coefficient of variation of 0.33, which was the preferable circumstance.

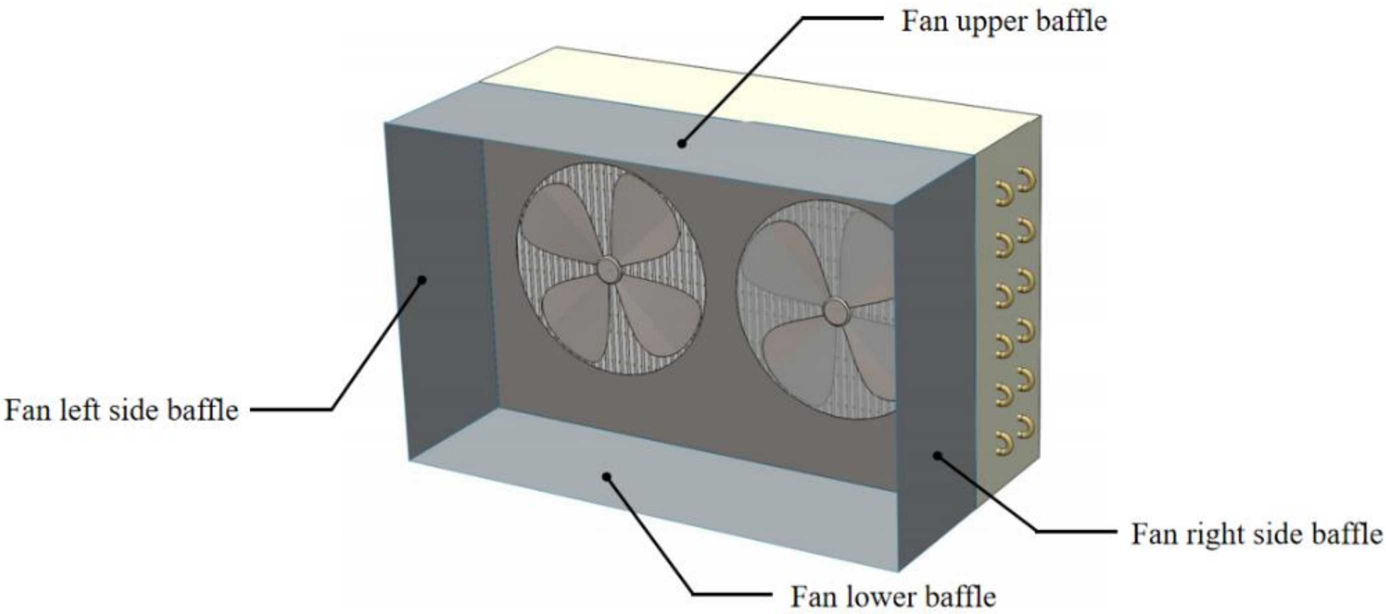

Figure 17. Arrangement diagram of FCU system with fan outlet baffle.

Table 5. Summary of the coefficients of variation of horizontal velocity profile for different fan baffle shapes.

Emulated Scenarios	Upper and Lower Opening Angle (°)	Left and Right Opening Angle (°)	Coefficient of Variation
Case 1	0	15	0.34
Case 2	0	30	0.43
Case 3	0	45	0.39
Case 4	0	60	0.33
Case 5	15	0	0.61
Case 6	15	15	0.48
Case 7	15	30	0.49
Case 8	15	45	0.48
Case 9	15	60	0.47
Case 10	30	0	0.80
Case 11	30	15	0.73
Case 12	30	30	0.69
Case 13	30	45	0.63
Case 14	30	60	0.58

The velocity distribution contours of the vertical and horizontal profiles in case 4 are shown in Figures 18 and 19, which were similar to the flow characteristics in Section 3.3.2; hence, the identical features were not repeated. The feature that differed from Section 3.3.2 was that the fan outlet baffle shape was adjusted to a flared shape, thereby expanding the airflow dispersion out of the outlet again. Figure 18 also indicated that the maximum velocities of both planes A and B increases from 0.98 m/s and 0.77 m/s to 1.22 m/s and 0.92 m/s, respectively, compared to Figure 15. Although optimizing the diffuser baffle shape did not significantly improve the average velocity in the vertical profile, the velocity stratification was more homogenous in the horizontal height, which indirectly confirmed the necessity of the vent shape optimization.

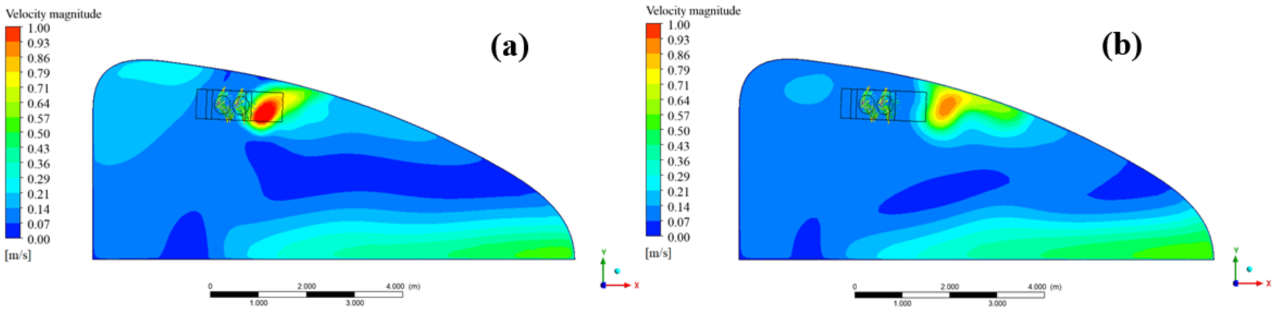

Figure 18. Velocity distribution contours for vertical profiles when the side opening angle was 60°: plane A (**a**) and plane C (**b**).

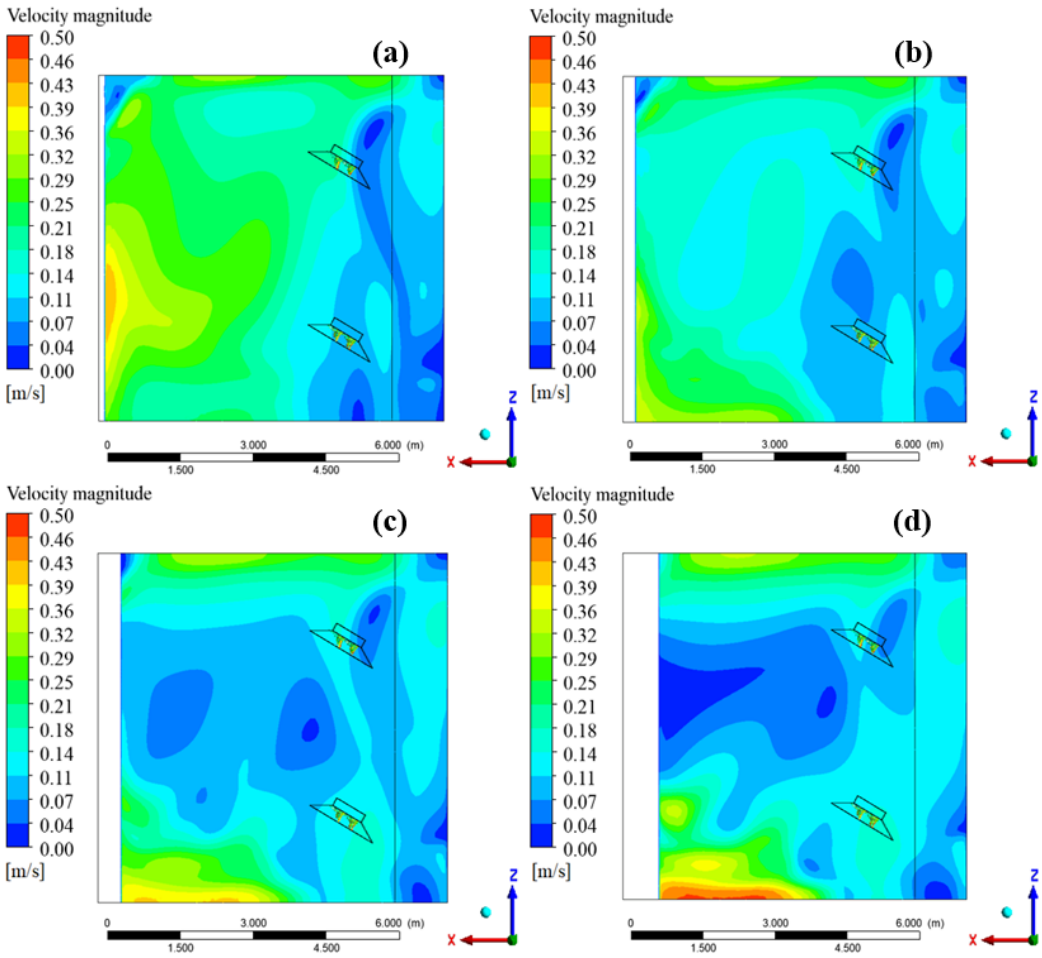

Figure 19. Velocity distribution contours for four horizontal profiles when the side opening angle was 60°: plane 1—0.7 m (**a**), plane 2—1.0 m (**b**), plane 3—1.3 m (**c**), and plane 4—1.6 m (**d**).

4. Results and Discussion

Based on the validated simulation model, the proposed layout parameters were determined systematically. The optimization results showed that the best uniform airflow field was formed when the fan tilt angle was −2.5°, the fan swing angle was 60°, the fan height above the ground was 2.9 m, and the side opening angle was 60°.

4.1. Analysis of Coefficient of Variation

For the proposed and traditional empirical system layouts, changing the placement strategy of the FCU systems would influence the overall uniformity as shown in Table 6. The variation regularity of the coefficient of variation when the system layout was not optimized could be expressed in the range of 0.63–0.91. This occurred as the fan was tilted upwards, and the circulating airflow blew directly from the outlet to the front of the greenhouse film then gradually down the film to the bottom corner of the south side as also seen clearly in Figure 9. Therefore, the concentration of the plane velocity in the south zone of the greenhouse was stronger as the horizontal height rose compared to the north side, where there was no significant airflow organization. This pattern of air circulation distribution led to extremely poor uniformity.

Table 6. Comparison of coefficients of variation for the proposed and traditional empirical system layouts.

Fan Height above the Ground (m)	Coefficient of Variation	
	Empirical Scheme	Proposed Scheme
0.7	0.63	0.43
1.0	0.72	0.25
1.3	0.77	0.22
1.6	0.91	0.44
Average value	0.76	0.33

In the proposed optimization scheme based on the simulation model, the variation regularity of the coefficient of variation could be expressed in the range of 0.22–0.44. There was a stable prevailing airflow at a level of 1.6 m from the ground, which resulted in the highest coefficient of variation and the worst uniformity. However, compared with the empirical layout, the coefficient of variation of this canopy plane decreased from 0.91 to 0.44, and the uniformity improved by 51.65%. The monitoring plane that was 0.7 m from the ground was closest to the greenhouse soil, and the airflow organization was unstable because the vortical flow fields acted in a complicated manner. Meanwhile, the uniformity at 1 m and 1.3 m from the ground also improved significantly. Therefore, the proposed system layout strategy facilitated the improvement of the crop microclimate, with the average coefficient of variation reduced from the conventional 0.76 to 0.33, and its overall uniformity in the canopy area improved by 56.58%.

The main purpose of the circulation fan applied in the CSG earlier was to provide a certain airflow for the crops [19,20]. However, there were few detailed studies on the effect of the installation factors of the circulation fans. This paper used ANSYS Fluent 2020 R1 to optimize the installation factors of the FCU systems based on the research of the literature [23–26] to seek a scheme that could form a more uniform airflow field. The coefficient of variation was used as a quantitative evaluation index to compare the airflow field homogeneity of different schemes. The results showed that the optimized scheme had a great improvement in the uniformity of the airflow field. It could guide the installation of FCU systems and could also provide a new idea for optimizing the greenhouse microclimate.

4.2. Analysis of Disturbance Characteristics of the Optimized System Layout

The disturbance characteristics of the optimized system layout were evaluated using the percentage of the velocity distribution in the different horizontal profiles as shown in Table 7. Zhuang et al. [21] used a wind speed range between 0.15 m/s and 0.50 m/s as the effective disturbance airflow. In this paper, we referred to this wind speed range and mainly analyzed the percentage of the airflow velocity distribution that was in this range. Table 7 demonstrates that the airflow velocity range before and after optimization was mostly distributed below 0.35 m/s. This was mainly because the fan rotation speed in the FCU systems was low and because the air supply was small; thus, the overall velocity level of the greenhouse was in a moderate range. The four horizontal planes before and after optimization were compared sequentially. It could be found that the percentages of planes 1 and 2 in the range of the effective disturbance airflow speed after optimization (58.68% and 43.73%) were improved compared with the empirical scheme (42.73% and

41.02%) and that plane 1 had the best enhancement effect. Meanwhile, the improvement of the effective disturbance airflow speed in planes 3 and 4 was not significant. This reason could be analyzed through the uniformity of the velocity distributions in the four horizontal profiles. As shown in Table 6, the velocity uniformity of plane 1 was the best among the four planes when unoptimized. It was more conducive to the formation of the effective disturbance wind speed when optimizing the uniformity, and plane 2 was the same. The velocity uniformity of planes 3 and 4 was poor before being optimized, while, with the optimized results of the coefficient of variation, it could be seen that the optimization effect of these two planes was relatively better. This was because the air supply volume of the system was constant, and a better disturbance speed could not be guaranteed while improving the uniformity. Therefore, the average velocity of planes 3 and 4 was in the relatively lower-speed range. This problem could be improved by adjusting the air supply volume of the FCU systems in the future.

Table 7. Comparison of percentages of velocity distribution for the proposed and traditional empirical system layouts.

Airflow Velocity (m/s)	Empirical Scheme (%)				Proposed Scheme (%)			
	Plane 1	Plane 2	Plane 3	Plane 4	Plane 1	Plane 2	Plane 3	Plane 4
<0.15	57.63	58.98	56.61	57.14	41.32	56.27	67.59	65.9
0.15–0.25	28.72	23.33	24.23	23.44	32.26	26.69	16.88	15.24
0.25–0.35	13.17	13.87	12.73	12.91	20.32	17.04	10.13	12.88
0.35–0.45	0.48	3.82	5.9	4.58	6.09	0	5.04	3.32
>0.45	0	0	0.53	1.93	0	0	0	2.61

Zhuang et al. and Zhang et al. [21,22] analyzed the installation height of the circulation fans in a CSG using the percentage of the velocity distribution as a quantitative evaluation index. However, the effects of other installation factors on the internal airflow field of the CSG have not been studied in depth. This paper analyzed the percentage of the velocity distribution after optimizing the four installation factors and compared the airflow velocity distribution range formed by the proposed and empirical schemes. The results of the optimized wind speed distribution percentages showed that the scheme proposed in this paper has the potential to improve the effective disturbance wind speed range while ensuring the optimized uniformity. Therefore, by comparing the percentage and coefficient of variation of the airflow velocity distribution, it could be concluded that the uniformity of the airflow field was considerably improved and that the disturbance effect of the system was improved to a certain extent when the four installation factors of the fan were optimized.

5. Conclusions

In this study, in order to solve the dilemma that various environmental parameters in solar greenhouses are less homogeneous, the numerical simulation method was used to analyze the airflow environment generated by a fan–coil unit (FCU) system in a greenhouse. Four critical installation parameters, the fan tilt angle, fan swing angle, fan height above the ground, and fan outlet baffle shape, were optimized to establish a uniform airflow field.

The greenhouse airflow organization before optimization was mainly concentrated in the south area with a high velocity, while the airflow velocity near the north side was very small and uneven. In addition, there was no significant airflow disturbance between the two identical fans. The overall coefficient of variation for the horizontal profiles was 0.76. The effective percentages of the airflow disturbance velocity in horizontal planes 1 and 2 were 42.73% and 41.02%, respectively. Based on the validated simulation model, the proposed layout parameters were determined systematically. The optimization results showed that the best uniform airflow field was formed when the fan tilt angle was $-2.5°$, the fan swing angle was 60°, the fan height above the ground was 2.9 m, and the side opening angle was 60°. The airflow velocity near the greenhouse's north side increased significantly, and the airflow disturbance at the crop canopy height was enhanced to a certain extent. The average coefficient of variation was reduced to 0.33, and its overall uniformity in the canopy area improved by 56.65%. The effective percentages of the airflow disturbance velocity in horizontal planes 1 and 2 were enlarged to 58.68% and 43.73%. The active multifunctional fan–coil system achieved a stable airflow transition without any additional devices or energy requirements, confirming the dominant role of the proposed installation parameters in the coefficient of variation and homogeneous characteristics and thereby generating a suitable thermal environment for the horticulture facility.

This paper provided a solution for improving the airflow field in Chinese solar greenhouses based on the proposed FCU system. The method for constructing the fan model is universal and can be applied to different types of greenhouse facilities. The optimization results are applicable to low-growing leafy vegetables. This paper contributed to guiding the installation of the FCU system and provided theoretical guidance for the optimization of the airflow field. The future development direction of this study is to consider the effect of different crop heights and growth stages on the airflow field. It is also necessary to further optimize and scientifically design an FCU system associating the temperature and airflow fields.

Author Contributions: Conceptualization, W.S.; Methodology, J.L. and H.L.; Software, J.L. and H.L.; Investigation, J.L., H.L. and C.Z.; Resources, S.Z.; Data curation, J.L.; Writing—original draft, J.L.; Writing—review & editing, H.L., X.H. and W.S.; Supervision, S.Z.; Project administration, W.S.; Funding acquisition, S.Z. and W.S. All authors have read and agreed to the published version of the manuscript.

Funding: This research was funded by the Natural Science Foundation of China (U20A2020) and the China Agriculture Research System of MOF and MARA (CARS-23-D02).

Data Availability Statement: Not applicable.

Conflicts of Interest: The authors declare no conflict of interest.

References

1. Tong, G.; Chen, Q.; Xu, H. Passive solar energy utilization: A review of envelope material selection for Chinese solar greenhouses. *Sustain. Energy Technol. Assess.* **2022**, *50*, 101833. [CrossRef]
2. Cao, K.; Xu, H.; Zhang, R.; Xu, D.; Yan, L.; Sun, Y.; Xia, L.; Zhao, J.; Zou, Z.; Bao, E. Renewable and sustainable strategies for improving the thermal environment of Chinese solar greenhouses. *Energy Build.* **2019**, *202*, 109414. [CrossRef]
3. Kitaya, Y.; Shibuya, T.; Yoshida, M.; Kiyota, M. Effects of air velocity on photosynthesis of plant canopies under elevated CO2 levels in a plant culture system. *Adv. Space Res.* **2004**, *34*, 1466–1469. [CrossRef] [PubMed]
4. Kitaya, Y.; Tsuruyama, J.; Shibuya, T.; Yoshida, M.; Kiyota, M. Effects of air current speed on gas exchange in plant leaves and plant canopies. *Adv. Space Res.* **2003**, *31*, 177–182. [CrossRef]
5. Li, H.; Ji, D.; Hu, X.; Xie, T.; Song, W.; Tian, S. Comprehensive evaluation of combining CFD simulation and entropy weight to predict natural ventilation strategy in a sliding cover solar greenhouse. *Int. J. Agric. Biol. Eng.* **2021**, *14*, 213–221. [CrossRef]
6. Kimura, K.; Yasutake, D.; Miyoshi, Y.; Yamanami, A.; Daiou, K.; Ueno, H.; Kitano, M. Leaf boundary layer conductance in a tomato canopy under the convective effect of circulating fans in a greenhouse heated by an air duct heater. *Environ. Control Biol.* **2016**, *54*, 171–176. [CrossRef]
7. Yasutake, D.; Yu, X.; Asano, T.; Ishikawa, M.; Mori, M.; Kitano, M.; Ishikawa, K. Control of greenhouse humidity and airflow with fogging and circulation systems and its effect on leaf conductance in cucumber plants. *Environ. Control Biol.* **2014**, *52*, 101–105. [CrossRef]
8. Walker, J.N.; Duncan, G.A. Effectiveness of Recommended Greenhouse Air Circulation Systems. *Trans. ASAE* **1974**, *17*, 0371–0374. [CrossRef]
9. Chen, J.; Xu, F.; Tan, D.; Shen, Z.; Zhang, L.; Ai, Q. A control method for agricultural greenhouses heating based on computational fluid dynamics and energy prediction model. *Appl. Energy* **2015**, *141*, 106–118. [CrossRef]
10. Fernandez, J.E.; Bailey, B.J. The Influence of Fans on Environmental Conditions in Greenhouses. *J. Agric. Eng. Res.* **1994**, *58*, 201–210. [CrossRef]
11. Ishii, M.; Okushima, L.; Moriyama, H.; Furihata, Y. Influence of Circulation Fans on the Distribution of Air Temperature and Air Velocity in a Greenhouse. *Shokubutsu Kankyo Kogaku* **2012**, *24*, 193–200. [CrossRef]

12. Tokairin, T.; Sumi, A.; Shimomura, N.; Kumazaki, T.; Suzuki, K.; Saigusa, M. Effect of Air Circulator on Airflow Distributions in Greenhouse with a Pad-Fan Evaporative Cooling System. *Shokubutsu Kankyo Kogaku* **2017**, *29*, 17–25. [CrossRef]
13. Tokairin, T.; Sumi, A.; Kumazaki, T.; Suzuki, K. Effect of airflow control on temperature distributions in a greenhouse with a fan-and-pad evaporative cooling system. *Acta Hortic.* **2018**, *1227*, 115–122. [CrossRef]
14. Baek, M.-S.; Kwon, S.-Y.; Lim, J.-H. Improvement of uniformity in cultivation environment and crop growth rate by hybrid control of air flow devices. *J. Cent. South Univ.* **2015**, *22*, 4702–4708. [CrossRef]
15. Baek, M.-S.; Kwon, S.-Y.; Lim, J.-H. Improvement of the Crop Growth Rate in Plant Factory by Promoting Air Flow inside the CultivationImprovement of the Crop Growth Rate in Plant Factory by Promoting Air Flow inside the Cultivation. *Int. J. Smart Home* **2016**, *10*, 63–74. [CrossRef]
16. Xu, J.; Li, Y.; Wang, R.Z.; Liu, W.; Zhou, P. Experimental performance of evaporative cooling pad systems in greenhouses in humid subtropical climates. *Appl. Energy* **2015**, *138*, 291–301. [CrossRef]
17. Hong, Y.; Wang, X.; Li, L.; Chen, J.; Lu, Q. CFD Simulation for Effect of Circulation Fans Arrangement on Flow Field in Greenhouse. *J. Agric. Mech. Res.* **2018**, *41*, 180–185. (In Chinese)
18. Chalill, S.M.; Chowdhury, S.; Karthikeyan, R. Prediction of Key Crop Growth Parameters in a Commercial Greenhouse Using CFD Simulation and Experimental Verification in a Pilot Study. *Agriculture* **2021**, *11*, 658. [CrossRef]
19. Duan, M.; Yang, F.; Wang, R.; Han, F.; Diao, L.; Xia, S. The Research of the Temperature in Solar Greenhouse in Winter. *J. Agric. Mech. Res.* **2014**, *36*, 54–57. (In Chinese)
20. Wang, R.; Duan, M.; Yang, F.; Yao, Y.; Zhang, W.; Li, Y. Study on temperature optimization in solar greenhouse in winter. *J. Northeast Agric. Univ.* **2014**, *45*, 101–106. (In Chinese)
21. Zhuang, Y.; Zhang, Y.; Zhao, S.; Song, W.; Ma, C.; Chen, X.; Zhang, T. Air-circulator effects on the greenhouse environment and tomato photosynthetic parameters in a Chinese solar greenhouse. *Acta Hortic.* **2018**, *1227*, 197–204. [CrossRef]
22. Zhang, Y.; Feng, X.; Shumei, Z.; Wang, Q.; Ren, X. Effects of Air Circulator on Environmental Parameter and Tomato Growth in Solar Greenhouse. *China Veg.* **2016**, *9*, 52–57.
23. Li, M.; Geng, R.; Song, W.; Wang, P.; Li, H.; Wang, X. Performances of Thermal Collecting and Releasing System Developed with Fan-coil Units in Plastic Tunnel Covered with Thermal Blanket. *Nongye Jixie Xuebao/Trans. Chin. Soc. Agric. Mach.* **2020**, *51*, 371–378.
24. He, X.; Wang, P.; Song, W.; Wu, G.; Ma, C.; Li, M. Experimental study on the feasibility and thermal performance of a multifunctional air conditioning system using surplus air thermal energy to heat a Chinese solar greenhouse. *Renew. Energy* **2022**, *198*, 1148–1161. [CrossRef]
25. He, X.; Wang, P.; Li, M.; Song, W. Parameters Optimization of Greenhouse Air-cooled Condenser Heat Collection and Release System by Response Surface Method. *Nongye Jixie Xuebao/Trans. Chin. Soc. Agric. Mach.* **2020**, *51*, 315–323.
26. Zong, C.; Wang, P.; Chen, X.; Li, M.; He, X.; Wang, J.; Xu, D.; Song, W. Influences of air thermal energy utilization system with fan-coil units on the thermal and humid environment of multi-span tunnel in cold wave. *Nongye Gongcheng Xuebao/Trans. Chin. Soc. Agric. Eng.* **2021**, *37*, 214–221.
27. Bournet, P.-E.; Rojano, F. Advances of Computational Fluid Dynamics (CFD) applications in agricultural building modelling: Research, applications and challenges. *Comput. Electron. Agric.* **2022**, *201*, 107277. [CrossRef]
28. Xie, S.; Zheng, J.; Xiao, B.; Hu, H.; Cao, X.; Wang, X.; Zhang, L. Numerical Simulation and Wind Tunnel Test on the Wind-Induced Response of Three Typical Types of Greenhouse Main Structures. *Agriculture* **2022**, *12*, 1294. [CrossRef]
29. Zhang, Y.; Kacira, M.; An, L. A CFD study on improving air flow uniformity in indoor plant factory system. *Biosyst. Eng.* **2016**, *147*, 193–205. [CrossRef]
30. Zhang, Y.; Kacira, M. Analysis of climate uniformity in indoor plant factory system with computational fluid dynamics (CFD). *Biosyst. Eng.* **2022**, *220*, 73–86. [CrossRef]
31. Posner, J.D.; Buchanan, C.R.; Dunn-Rankin, D. Measurement and prediction of indoor air flow in a model room. *Energy Build.* **2003**, *35*, 515–526. [CrossRef]
32. Li, H.; Li, Y.; Yue, X.; Liu, X.; Tian, S.; Li, T. Evaluation of airflow pattern and thermal behavior of the arched greenhouses with designed roof ventilation scenarios using CFD simulation. *PLoS ONE* **2020**, *15*, e0239851. [CrossRef] [PubMed]
33. Zhang, Y. Improving Climate Uniformity and Energy Use Efficiency in Controlled Environment Agriculture. Ph.D. Thesis, The University of Arizona, Tucson, AZ, USA, 2019.
34. Yeo, U.-H.; Lee, S.-Y.; Park, S.-J.; Kim, J.-G.; Choi, Y.-B.; Kim, R.-W.; Shin, J.H.; Lee, I.-B. Rooftop Greenhouse: (1) Design and Validation of a BES Model for a Plastic-Covered Greenhouse Considering the Tomato Crop Model and Natural Ventilation Characteristics. *Agriculture* **2022**, *12*, 903. [CrossRef]
35. Bouhoun Ali, H.; Bournet, P.E.; Cannavo, P.; Chantoiseau, E. Development of a CFD crop submodel for simulating microclimate and transpiration of ornamental plants grown in a greenhouse under water restriction. *Comput. Electron. Agric.* **2018**, *149*, 26–40. [CrossRef]
36. Boulard, T.; Roy, J.C.; Pouillard, J.B.; Fatnassi, H.; Grisey, A. Modelling of micrometeorology, canopy transpiration and photosynthesis in a closed greenhouse using computational fluid dynamics. *Biosyst. Eng.* **2017**, *158*, 110–133. [CrossRef]

37. Benni, S.; Tassinari, P.; Bonora, F.; Barbaresi, A.; Torreggiani, D. Efficacy of greenhouse natural ventilation: Environmental monitoring and CFD simulations of a study case. *Energy Build.* **2016**, *125*, 276–286. [CrossRef]
38. Villagrán, E.A.; Baeza Romero, E.J.; Bojacá, C.R. Transient CFD analysis of the natural ventilation of three types of greenhouses used for agricultural production in a tropical mountain climate. *Biosyst. Eng.* **2019**, *188*, 288–304. [CrossRef]